INTERFACE

royalsocietypublishing.org/journal/rsif

Research

Cite this article: Kunrath MF, Vargas ALM, Sesterheim P, Teixeira ER, Hubler R. 2020 Extension of hydrophilicity stability by reactive plasma treatment and wet storage on TiO_2 nanotube surfaces for biomedical implant applications. *J. R. Soc. Interface* **17**: 20200650. http://dx.doi.org/10.1098/rsif.2020.0650

Received: 11 August 2020
Accepted: 1 September 2020

Subject Category:
Life Sciences–Engineering interface

Subject Areas:
biomaterials, biomedical engineering, nanotechnology

Keywords:
anodization, biocompatibility, surfaces, biomedical implants, hydrophilicity, TiO_2 nanotubes

Author for correspondence:
Marcel F. Kunrath
e-mail: marcelfkunrath@gmail.com

THE ROYAL SOCIETY PUBLISHING

Extension of hydrophilicity stability by reactive plasma treatment and wet storage on TiO_2 nanotube surfaces for biomedical implant applications

Marcel F. Kunrath[1,2], André L. M. Vargas[2], Patrícia Sesterheim[3], Eduardo R. Teixeira[1] and Roberto Hubler[2]

[1]Dentistry Department, School of Health and Life Sciences, Pontifical Catholic University of Rio Grande do Sul (PUCRS), Av. Ipiranga, P.O. Box 6681, 90619-900, Porto Alegre - RS, Brazil
[2]Materials and Nanoscience Laboratory, Pontifical Catholic University of Rio Grande do Sul (PUCRS), P.O. Box 1429, 90619-900, Porto Alegre - RS, Brazil
[3]Institute of Cardiology, R. Domingos Crescencio, P.O. Box 132, 90650-090, Porto Alegre - RS, Brazil

MFK, 0000-0003-0493-8891; RH, 0000-0002-8625-5607

Micro and nanoscale changes allow the optimization of physico-chemical properties of titanium implant surfaces. Recently UV and plasma treatments have allowed surface hydrophilicity to take increased prominence; however, this beneficial effect is short-lived. The aim of this study is to investigate methodologies post-anodizing treatment to generate and maintain high surface hydrophilicity along with high biocompatibility. Anodized surfaces were characterized regarding physical–chemical properties. Then, surface wettability with nanomorphology was evaluated at different times and with distinct post-treatments: as deposited, with a reactive plasma and UV-light post-treatment, stored in air or deionized (DI) water. Adhesion, alkaline phosphatase (ALP) activity and bone cell viability tests were executed after the incremental treatments. The anodizing process generated a surface with TiO_2 nanotubes morphology and micro-roughness. Plasma-treated surfaces resulted in the most hydrophilic samples and this property was maintained for a longer period when those were stored in DI water (angle variation of 7° to 12° in 21 days). Furthermore, plasma post-treatment changed the titanium surface crystalline phase from amorphous to anatase. Anodized surfaces modified by reactive plasma and stored in DI water suggest better hydrophilicity stability, biocompatibility, ALP activity and achievement of crystalline phase alteration, indicating future potential use on biomedical implants.

1. Introduction

Orthopaedic and dental implants are increasing in global prevalence, with hundreds of thousands of operations performed annually. However, a significant proportion of these operations fail (around 11% more) due to early loading by clinicians [1]. Thus, researchers are proposing several modifications to surface topography and chemical activity of the titanium-based implants in order to promote higher biocompatibility, fast cell adhesion and physical–chemical resistance [2–4]. Dental and orthopaedic titanium implants are submitted to post-processing treatments and surface texturizing to accelerate and improve cell reaction along the surface in order to provide faster and more effective bone adhesion [5,6].

Titanium surface treatments alter many properties, such as morphology, roughness, crystalline phase and wettability [3,5,6]. These properties strongly influence the cellular responses [2,5,6] and need to be evaluated with rigorous characterization tests every time a new implant surface is proposed. Electrochemical anodization possesses a characteristic of creating a surface morphology with

TiO_2 nanotubes (TNTs), which present a characteristic of superficial large area nanotexturization [6,7]. TNTs possess unique surface properties such as the ability to carry drugs or nanoparticles, to increase surface energy, to alter wettability and to interact with cells at the nanoscale [7–10], which can improve the success rate of biomedical implants.

Wettability is one of the properties most reported by researchers with degradations due to ageing occurring in the storage environment [11]. Scharnweber *et al*. [11] reported that atmospheric organic impurities contaminate the surfaces of the titanium implant during shelf storage and reduce the adhesion of plasma proteins and osteoblasts. On the other hand, expressive wettability alterations are made with post-TNTs manufacturing treatments [12]. Recent approaches with thermal treatments, photofunctionalizations, UV and plasma usage, and coating applications [8,12–15] presented substantial wettability alterations of the TNTs, both for hydrophilic and hydrophobic properties. Choi *et al*. [10] reported that UV and plasma treatment increased the rates of attachment, spread and proliferation of murine osteoblast cells, as well as the capacity of protein adsorption. Similarly, other studies have proposed the application of UV-light to increase hydrophilicity and consequently obtained improvements in cell responses that are determinants for faster osseointegration [16,17]. However, many of these treatments quickly alter the wettability without the possibility of maintaining these enhanced properties for an extended period of time after contact with air [11,13].

Highly hydrophilic properties are reported by studies to have greater adhesion potential and cell proliferation in biomedical implants due to their high-energy surface and cell spread [14,18]. As such, surface nanotexturization shows more expressive results in osteogenic evolution and proliferation speed in *in vitro* and *in vivo* studies [6,9,19]. Some authors reported that TNTs present an amorphous crystalline phase after deposition and thermal annealing converts the surface to the anatase phase and promotes enhanced biocompatibility between the TNTs and osteogenic cells [20,21]. In addition, expressive benefits are evidenced in relation to cellular responses when the topographic orientation has characteristics in a highly oriented or partially oriented design [22]. These results show that these optimized properties should be available at the time of surgery without losing these characteristics during manufacturing, storage and sale of biomedical implants.

In this work, we report the development of a nanostructured surface (TNTs) from an anodizing treatment over pure titanium grade II in order to evaluate its physical–chemical and bio-adhesion properties. Moreover, investigation of methodologies such as reactive plasma, UV-light exposure and deionized (DI) water storage, aiming to alter and maintain surface hydrophilicity up to 21 days. Finally, the changes in the crystalline phase and superficial morphology on surfaces, along with biocompatibility and cell adhesion tests were analysed.

2. Materials and methods

2.1. Samples preparation

A titanium grade II slate (TitanioBrasil, São Paulo, Brazil) was used to manufacture 50 discs, 1 mm thick and 6 mm wide. The samples were cleaned with a 70% ethanol solution (this and all other reagents were from Sigma, St Louis, MO, USA, unless otherwise indicated) and manually grounded using emery papers (SiC papers) of varying grit sizes (300, 600 and 900) to achieve a similar surface finish. To initiate the anodizing process, the samples were put in acetone for 5 min and then washed with DI water.

Table 1. Anodized groups (TNTs) and storage condition after first wettability test.

anodized groups (TNTs)	treatment after anodization	storage after immediate wettability test
G1 - TNTs	no treatment	ambient conditions - sterilized 24-well cell culture plate sealed
G2 - TNTs - UV	UV light for 10 min previous the wettability test	ambient conditions - sterilized 24-well cell culture plate sealed
G3 - TNTs - plasma	reactive plasma	ambient conditions - sterilized 24-well cell culture plate sealed
G4 - TNTs - plasma - DI	reactive plasma	deionized water - sterilized 24-well cell culture plate sealed

2.2. Anodizing process

All the samples were attacked with a solution of hydrochloric acid (HCl – 38%) and sulfuric acid (H_2SO_4) diluted at 70% for 1 h at 98°C in order to produce a rougher surface. The samples were washed as described: DI water, isopropylic ethanol, acetone and DI water. All reagents were purchased from Merck with the highest purity—PA (*pro analyse*) grade. After drying with dry nitrogen flux, the samples were anodized in an ultrasonic bath (25 kHz) with an electrolytic solution composed of ethylene glycol, 0.5% NH_4F (ammonium fluoride), 10% DI water and controlled voltage of 40 V for 1 h. The Ti samples were used as the anode and a Pt (platinum) sheet was used as the cathode. The temperatures of the solution and bath were maintained at 10°C during the entire process. After anodizing, the sample was cleaned with the same sequence and dried with N_2. The samples were divided into four groups as showed in table 1. A non-anodized surface was used as control. Finally, the samples were enveloped and sealed on sterilization paper, to be opened only when the characterization and wettability tests were performed.

2.2.1. Reactive plasma

For plasma treatment, a dedicated vacuum chamber was developed. The equipment consisted of a cathode with a central magnet oriented in the N–S direction and eight inverted orientation satellite magnets (S–N). The chamber was coupled to a vacuum system consisting of a diffusion pump (600 l s^{-1}) and a mechanical pump (22 m^3 h^{-1}) both Edwards brand. The cathode was machined from titanium and the anodized titanium samples were placed on it with the surface to be treated upwards. The anode consisted of a brass ring 2 mm away from the cathode in order to form the plasma only in the central region of the equipment as can be seen in figure 1. After mounting the equipment with the samples, the chamber was evacuated to a base pressure of 6×10^{-5} Pa. The system was filled with a mixture of 90% Ar (6.0) and 10% O_2 (5.0) up to a working pressure of 3×10^{-1} Pa. All gases were purchased from Air Products Company. To start the plasma an Advanced Energy DC power source

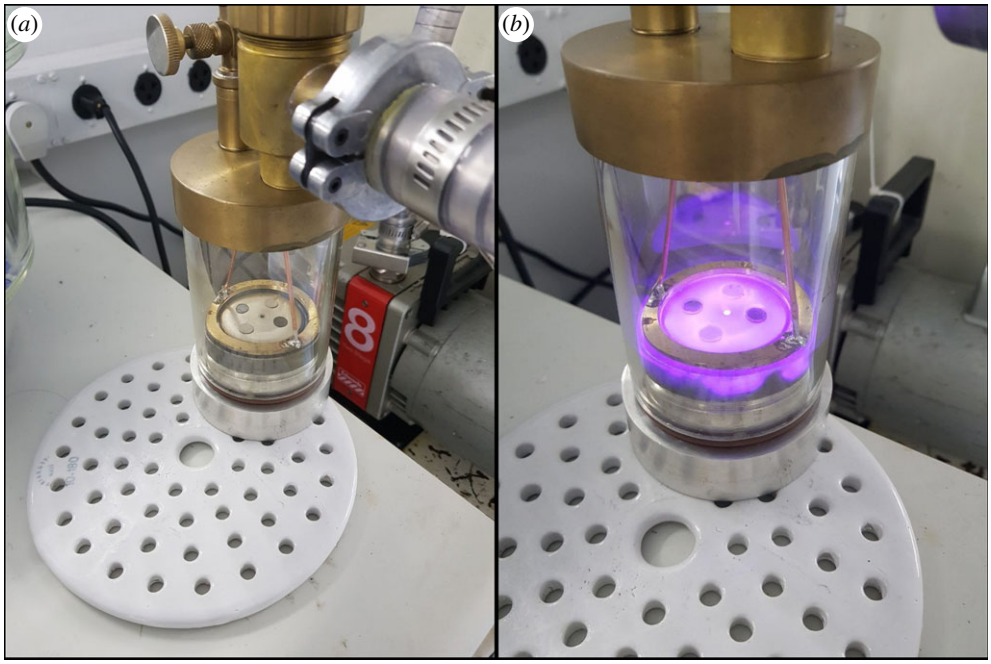

Figure 1. Device disconnected (*a*) and device in operation applying the plasma treatment (*b*).

operating at 400 V and a controlled power of 30 W was used. For all samples, the plasma application time was 5 min in order not to promote changes in the temperature of the samples. Figure 1 shows the device in operation.

When the plasma is on, the luminous region is formed by electrons and ions of Ar^{+}, Ar^{++}, $O_2{}^{+}$ and $O_2{}^{++}$. The positive ions are accelerated towards the cathode which is at a potential of −400 V resulting in energies between 400 and 800 eV. The energy of the ions will be transferred to the surface of the samples, generating surface annealing [23]. As the surface is formed by TiO_2 nanotubes, channelling will increase the range of the ions allowing the annealing to take place at a greater depth. This superficial annealing may precipitate crystalline phases in this region, which will be evaluated by X-ray diffraction.

2.2.2. Ultraviolet light treatment

For the post-anodizing UV light treatment (300 nm wavelength), a UV light chamber (QT-UV600-C, FL, USA) was used to put the samples ($n = 9$) inside for 10 min, based in short UV applications [24,25], for later surface characterization.

2.3. Surface characterization

To evaluate morphology and properties of the TiO_2 nanotubes acquired by the anodizing process, a scanning electron microscope (FESEM, Inspect F50, Prague, Czech Republic), a transmission electronic microscope (TEM, Tecnai G2 T20, Prague, Czech Republic), Rutherford backscattering spectroscopy (RBS, Tandetron 3 MV) and Raman Spectroscopy (Witec AlphaR-300) were used.

For roughness characterization, an atomic force microscope (AFM, Dimension Icon, Bruker, MA, USA) was used. Three readings were made in three different random samples ($n = 3$) at three different points (control samples and anodized samples), with the cut-off value of 30 µm, for statistical analysis using the NanoScopeAnalysis® software [26]. Two roughness parameters were measured (Ra—two-dimensional and Sq—three-dimensional).

The crystalline structure of each sample was investigated by X-ray diffraction (XRD; XRD-7000, Shimadzu). Cu-K_α radiation was used at 40 kV and 40 mA and the measurement were performed for 2θ values between 10° and 100° with a 0.02° pitch [14].

2.4. Wettability tests

To measure the wettability stability of anodized surface groups, a Goniometer—Contact Angle Measure (Phoenix 300, SEO, Kosekdong, Korea) was used. The test was applied at five different times: immediately after anodization (plasma or UV); 1 h, one week, 10 days and 21 days after the first measurement. All measurements were performed with three different samples for each time and group. A drop of 0.012 ml of DI water was applied on the surface and measured by the software (Surfaceware8, version 10.11, Korea). The samples were stored after the first test according to table 1.

2.5. Cell culture

For the biocompatibility tests, the surface treatments post anodization with the best hydrophilicity performance were chosen (G1 and G3, G4—groups using reactive plasma) to be compared with the negative control (machined surface). For a completely sterile environment, all samples were sterilized in a 120° autoclave for 30 min after the anodizing process, and the post-treatment applied previously to the cell culture experiments. The samples were transferred under sterile conditions and the cell experiment was carried out in a sterile flow chamber.

Epididymal adipose tissue of two male 8- to 10-week-old Lewis rats was used to collect adipose tissue-derived mesenchymal stem cells (ASCs). The present study was approved by the Ethics Committee for Animal Research of the Pontifical Catholic University of Rio Grande do Sul (protocol no. 7467) following all regulations for animal use (Brazilian Regulation no. 11.794, October 2008) according to Ethical Principles in Animal Experimental Research. Culture medium (CM) was composed of Dulbecco's modified Eagle's medium/low glucose (DMEM, Gibco BRL, Gaithersburg, MD, USA) with 3.7 g l^{-1} sodium bicarbonate (this and all other reagents were from Sigma, St Louis, MO, USA unless otherwise indicated), 2.5 g l^{-1} HEPES, 10% fetal bovine serum (Cultilab, SP, Brazil) and 1% penicillin/streptomycin (Gibco). Primary cultures were established by plating the cells into six-well culture plates (TPP, Trasadingen, Switzerland), with incubation at 37°C in with 5% CO_2, for 72 h. With 80% confluence, osteogenic differentiation was induced by culturing for four weeks in CM supplemented with 10–5 M dexamethasone,

5 µg ml^{-1} ascorbic acid 2-phosphate and 10 mM β-glycerophosphate [26,27], and ASCs in osteogenic medium alone were observed as control cultures. Differentiated osteoblasts (1×10^4 cm^{-2}) were seeded over the samples.

2.5.1. Viability

Osteoblast viability on different surfaces was ($n = 3$ per group and time) evaluated by 3-(4, 5-dimethylthiazol-2-yl)-2, 5-diphenyl tetra-zolium bromide (MTT, Sigma-Aldrich, São Paulo, Brazil) assay. After incubation for 3 and 10 days, the samples were washed with PBS and transferred into a new 96-well plate (TPP, Trasadingen, Switzerland). Next, the mixed solution of α-MEM (400 µl) and MTT (100 µl) was added. The solution was then cleared until the plate was put in a constant temperature incubator at 37°C for 4 h. Afterwards, 300 µl of dimethyl sulfoxide (DMSO) was added. Finally, 200 µl of DMSO solution was transferred to a 96-well plate, and the absorbance was measured with a spectrophotometric microplate reader at a wavelength of 490 nm [28].

2.5.2. Alkaline phosphatase

For alkaline phosphatase (ALP) activity measurements, osteoblasts were seeded into 24-well plates (TPP, Trasadingen, Switzerland), on four surface groups (control, G1, G3 and G4), and incubated at 37°C with 5% CO_2. After the culture time, the intracellular ALP was investigated at 3 and 10 days. Thereunto, centrifugation at 10 000 rpm for 5 min was applied, and the supernatant was collected for the detection of ALP activity. The final measurements were normalized using the total protein and calculated using a BCA (bicinchoninic acid) Protein Assay Kit (Pierce, Bonn, Germany), which was employed according to the manufacturer's instructions. Final absorbance was investigated using spectrophotometric microplate reader at 490 nm [28].

2.5.3. Adhesion

Osteoblasts were seeded into 24-well plates (TPP, Trasadingen, Switzerland), on four surface groups (control, G1, G3 and G4), and incubated at 37°C with 5% CO_2, for 240 h. Afterwards, samples ($n = 2$) were gently washed three times with 10 ml of phosphate-buffered saline to remove loosely bound cells and immediately fixed by immersion in 2.5% glutaraldehyde and 0.1 M phosphate buffer (pH 7.2–7.4) for 1 week. Samples were prepared by critical point drying and sputtered with gold to be examined using SEM at an accelerating voltage of 20 kV.

Furthermore, samples ($n = 2$) were stained using rhodamine B (100 nM) during 10 min of incubation in the dark at environment temperature, to visualize the cell nuclei. Rhodamine binds to cell DNA and fluorescence intensity may express cell number and vitality. The samples were rinsed with PBS three times and fixed with formaldehyde 4% for 30 min. Confocal microscopy (Zeiss, LSM 5 Exciter, Germany) was employed to visualize the cell staining.

2.6. Statistical analyses

All data are as means ± standard deviation (s.d.). For continuous data (roughness, wettability, MTT, ALP), comparisons between groups were applied using the Student's t-test. One-way ANOVA, when necessary, was applied to analyse the results. We performed statistical analysis using OriginPro 7.5 and a significant difference between groups was considered to occur at 5% ($p < 0.05$).

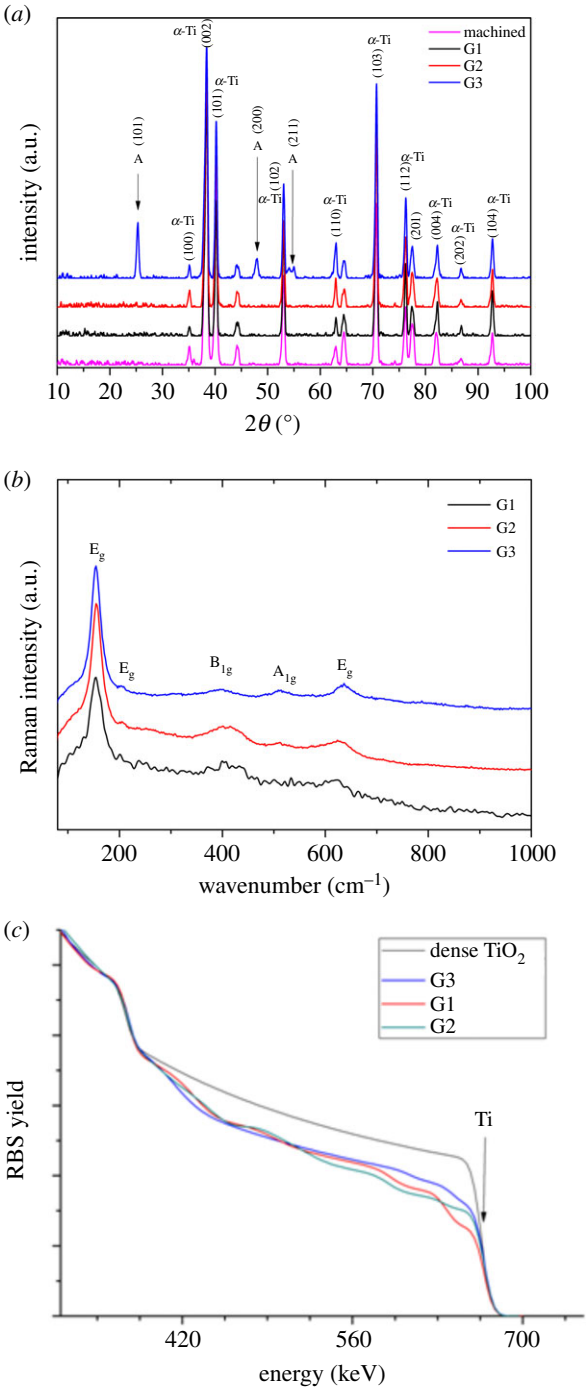

Figure 2. Surface properties of TNT samples from this work: (*a*) XRD spectra; (*b*) Raman spectra and (*c*) RBS spectra.

3. Results

3.1. Surfaces characterization

As soon as the samples were made, the crystal structure was characterized by grazing angle XRD (incidence angle of 3°). The XRD patterns, for all samples, exhibit peaks associated with the substrate material, Ti-machined, matching the alpha-titanium crystallography (PDF no. 44–1294), with the exception for the sample G3 from group figure 2*a*. The sample from group G3 shows four different peaks (indicated by arrows letter A) that match with the anatase crystal structure ($2\theta =$ 25.38°; 48.07°; 53.92°; 55.10°) matching the pattern PDF no. 21–1272. It shows that plasma treatment changed the crystalline structure of the TNT surface. Due to the high energy of the impacts of Ar and O_2 ions on the surface of the TNTs during

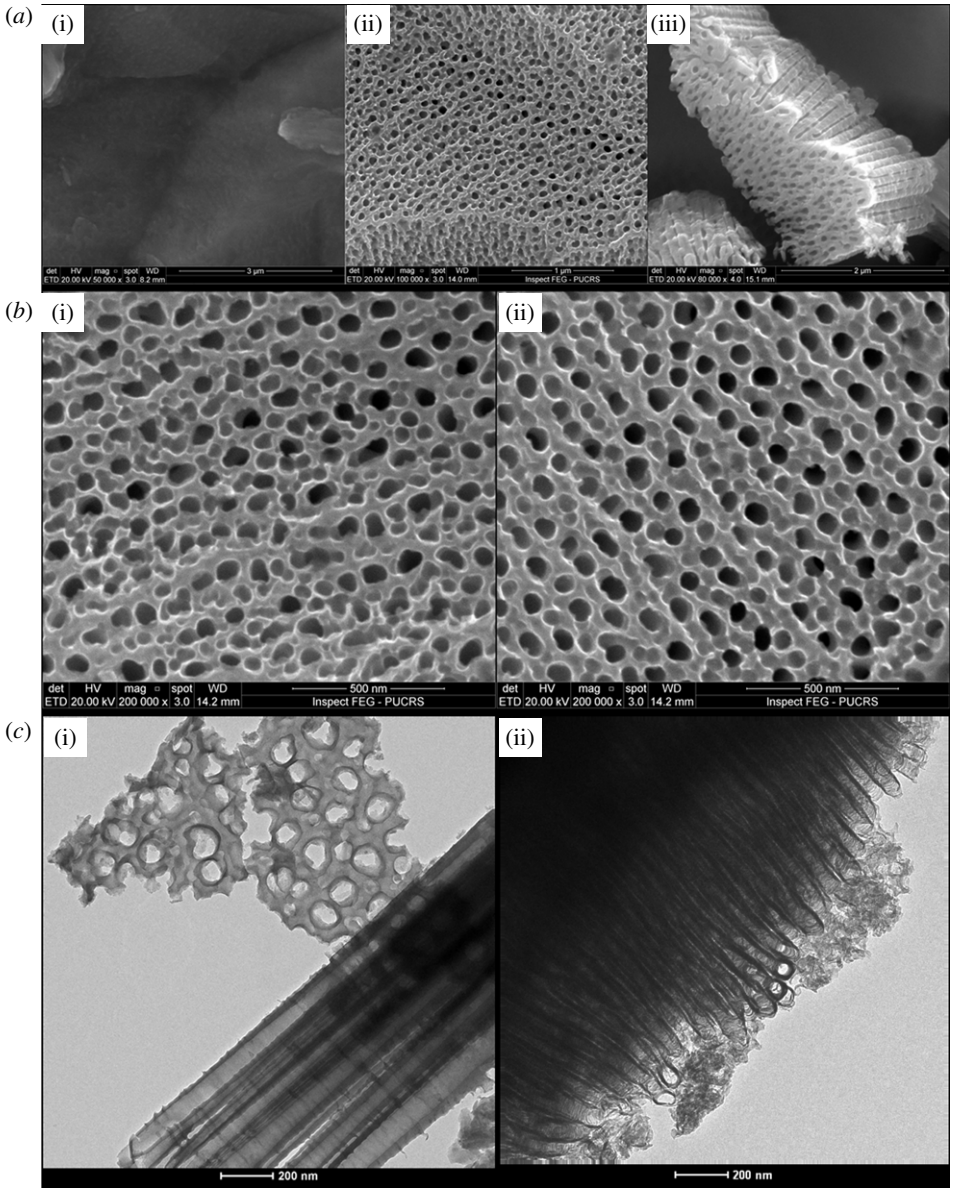

Figure 3. Superficial morphology of machined surface (*ai*) and superficial and lateral morphology of anodized surface (*a*ii, iii). Evaluation of surface morphology after UV-light (*b*i) and plasma (*b*ii) treatments. TEM of TiO_2 nanotubes (*c*).

the plasma treatment process, it is possible that the crystallization of the anatase phase has occurred. Anodizing of titanium surfaces revealed Raman vibration modes (figure 2*b*) at 155 cm^{-1} (Eg-A), 2020 cm^{-1} (Eg-A), 397 cm^{-1} (B1 g-A), 407 cm^{-1} (B1 g-A), 514 cm^{-1} (A1 g-A) and 636 cm^{-1} (Eg-A) belonging to the TiO_2 anatase phase [29–31]. This observation is consistent with X-ray diffraction data which revealed a mixture of the anatase phase with the compact hexagonal phase of the metallic Ti present in samples G1, G2 and G3.

Figure 2*c* shows the RBS spectrum obtained with 1 MeV alpha particle beam detected at an angle of 165°. The samples from groups G1, G2 and G3 were compared with a dense titanium oxide sample of the same thickness as the TNTs. It can be observed that samples with TNTs have a decrease in surface count due to density decrease due to nanotubes. Group G1 that received no post-treatment showed the largest decrease in counts, indicating the formation of nanotubes on the surface. The plasma exposure group G3 shows that there was an increase in surface density due to mixing caused by ion bombardment; however, still with a lower density than dense TiO_2, indicating that the structure of TNTs was not compromised. This increase in density may also be due to the formation of the anatase phase near the sample surface. The G2 group that received 10 min of UV radiation showed a slight increase in density compared to the G1 group probably caused by the higher surface oxidation due to UV exposure in air. Further details on the use of RBS for the characterization of TNTs can be found in reference [32].

The proposed anodizing process developed a nanostructured TNT surface as can be seen in figure 3*a*,*b*. No changes in surface morphology were observed after the use of UV light or reactive plasma (figure 3*b*). Table 2 shows the measurements made by FESEM, without statistical significance, between the nanotube's diameter and the intertubular spaces after the different treatments. Further details on the nanotube structures can be obtained from a previous study [32]. Transmission microscopy shows anodized tubes of high quality, with thick walls and an empty internal area, which increases surface energy (figure 3*c*).

The roughness measured by the AFM in the samples was statistically higher in the TNTs (in average 1570 nm) than in the control group (in average 210 nm) as observed in two

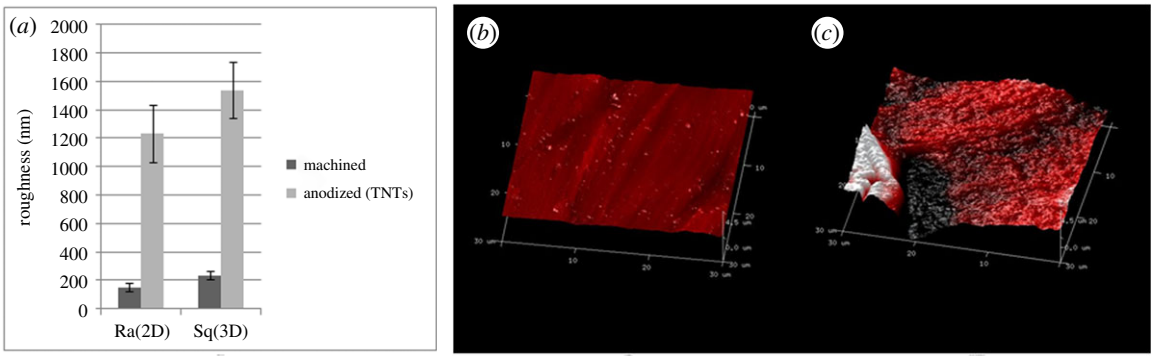

Figure 4. (*a*) Roughness measurements in two parameters (Ra and Sq) and three-dimensional graphs of machined surface (*b*) and anodized surface (*c*). Statistical significance is shown by $*p < 0.05$.

Table 2. Nanotubes diameter and intertubular spaces measures.

post-treatments	nanotubes diameter (nm)	intertubular distances (nm)
G1	66 ± 5.5	20.2 ± 18.5
G2	64.7 ± 7.5	25.2 ± 15
G3	68 ± 3.5	21.5 ± 20.2

analysis parameters: Ra (two-dimensional) and Sq (three-dimensional), which can be seen in figure 4.

3.2. Wettability stability

The wettability results show alterations of this property in relation to the post-treatment, time and storage condition. The best surface performances in terms of hydrophilicity are immediately verified after the application of plasma or UV light (figure 5*a*) with the lowest contact angle 7° in G4. As time elapses (1 h, 1 week, 10 days and 21 days), the stored samples in contact with air presented loss of hydrophilicity, while the group stored in DI water maintained constant hydrophilicity (figure 5*a*). Statistically, plasma and UV light post-anodizing intensely altered the surface hydrophilicity at time 0 h and 1 h ($*p < 0.05$). However, after 1 week and 10 days, only groups G3 and G4 presented significant data ($*p < 0.05$) and after 21 days, only group G4 maintained total hydrophilicity, as can be seen in the graphic (figure 5*b*).

3.3. Biological responses (viability, alkaline phosphatase and qualitative adhesion)

The viability of surface osteoblasts was investigated through a MTT test. G4 (TNTs + plasma + DI) was statistically superior both in 3 days as well as in 10 days compared to the machined surface (control) and TNTs without post-treatment (G1), $*p < 0.05$, revealing a better reaction and cell viability with the surface in the early periods (figure 6*a*). Similarly, in relation to ALP activity, the results of the group (G4) stored in DI water were statistically superior at 3 and 10 days. However, after 10 days, the group treated with plasma and stored in ambient O_2 (G3), showed the same performance suggesting a similar cell reaction after a long period of culture with bone cells (figure 6*b*).

In addition, after 10 days of culture, the qualitative microscopy images suggest excellent adhesion and well-marked osteoblastic tissue formation on the surface of the G4 group in relation to the other groups tested, which suggests a quicker and positive relation between cells and biomaterial (figure 7). However, the images suggest excellent adhesion in the G3 group, according to the qualitative analysis, and stable cell adhesion in the G1 and control groups.

4. Discussion

Seeking the development of an accessible surface for clinical use, we resorted to a methodology that promoted important physico-chemical surface modifications to the, Ti, including nanomorphology, high biocompatibility and superhydrofilicity in order to have the best biological response to bone cells. These three properties are individually reported through studies as surface changes that significantly improve cellular responses [2,9,13,14].

Thus, we critically characterize the anodized surface after additional UV light and Ar/O_2 plasma treatments to show its advantages in terms of biocompatibility. Surface nanomorphologies and changes in the crystalline phase (anatase) of Ti surfaces are proven promoters of better behaviour and cellular expression [9,21,33]. The application of Ar/O_2 plasma altered the crystalline phase of the Ti surface justifying the different peaks found in the XRD and Raman analyses corresponding to the anatase phase. Different surface heating methodologies are reported to modify the crystal structure of Ti such as thermal heating, cold plasma or ions bombardment [13,14,23,34]. Usually, the methodologies applied for the transformation of the crystalline phase use high temperatures and a greater amount of time, reporting minimal morphological changes or small volume reductions [35,36]. Moreover, the process of transforming from the amorphous phase to anatase is important for mechanical endurance. A previous study reported that initial fracture of the nanotubes occurs followed by subsequent densification, which improves the mechanical properties such as hardness and the elastic modulus [35]. All of these characteristics together promote topographic properties with better performance for application in a biological environment. The plasma methodology proposed in this study altered the crystalline phase of the surface within a short period (5 min), using a clean, high-vacuum process with low

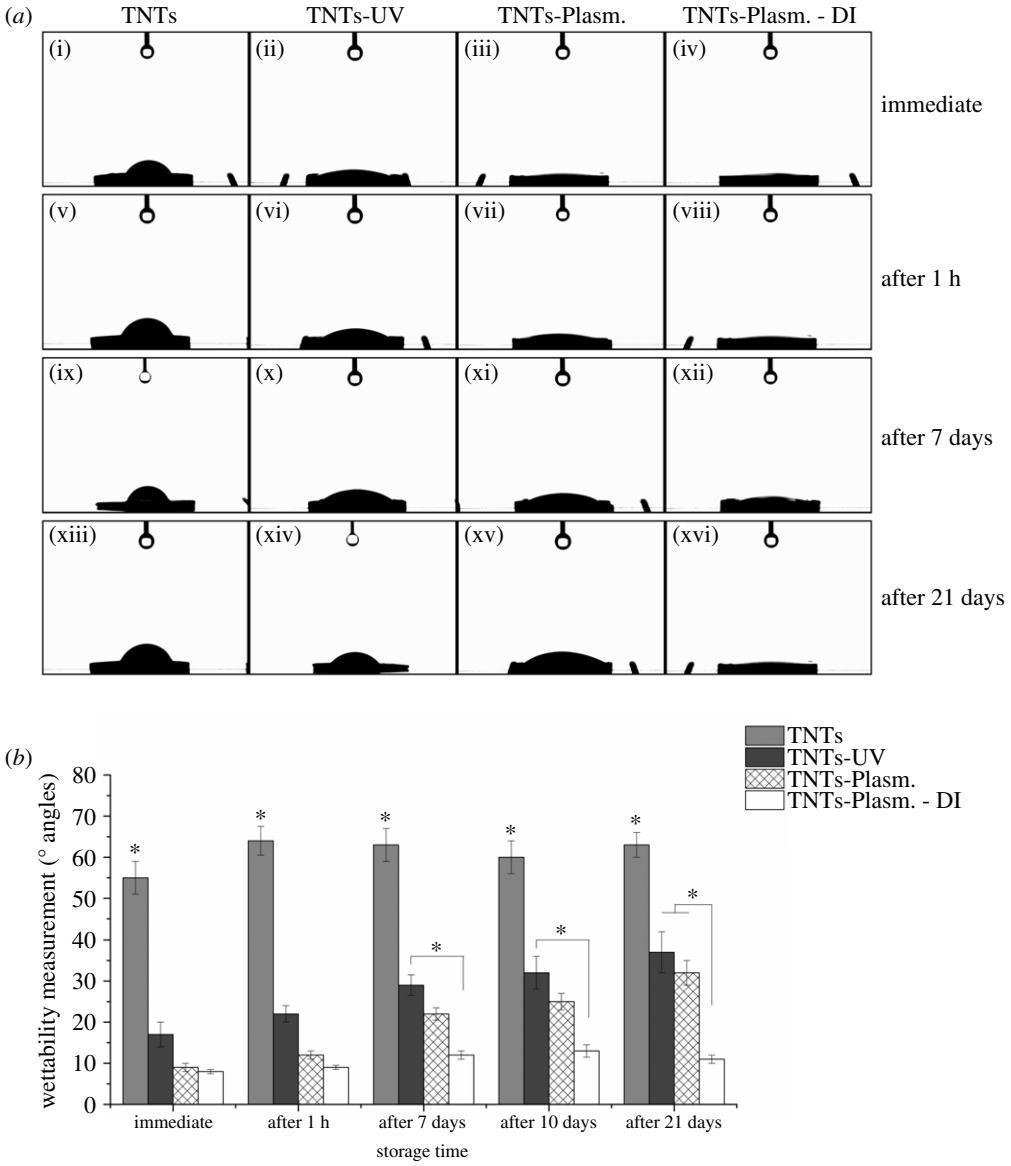

Figure 5. Wettability tests of different treatments after anodization at different analysis times (*a*). Graphs with statistical significance (*$p < 0.05$) comparing groups (*b*).

system heating (no more than 35°C) when compared to heat treatments.

Yu Sun *et al*. [13] altered the crystalline phase and wettability properties of Ti by heating in a muffle furnace. They concluded that the crystalline phase has an important influence on hydrophilicity properties as well as surface oxygen vacancy; however, the authors did not perform biological tests to assess cell interaction [13]. In a similar study, Roach *et al*. [37] characterized samples with TiO_2 nanotubes by XRD and showed higher bioactivity by simulated body fluid immersion in samples where the crystalline phase was anatase. Duske *et al*. [34] suggested a different plasma methodology and used a cold plasma model; their samples had high wettability change and their results showed better cell spreading on the superhydrophilic surfaces developed with plasma. The results of these studies corroborate our results using our novel plasma methodology.

The wettability of biomedical implants is the most discussed property by researchers because of its hydrophilic and hydrophobic advantages [11,12,38]. The application of plasma over the anodized surface produced superhydrophilic characteristics, which has been reported by many studies as being advantageous for adhesion, proliferation and bone differentiation [14,39,40]. However, titanium oxidation occurred in all post-anodizing treatments proposed, with small differences in maintenance over three weeks. Therefore, to increase hydrophilicity, it is necessary to use a solution that partiality inhibits the oxidation process by O_2, as is our proposal with DI water. Choi *et al*. [14] reported similar properties with the use of solutions around the surface. Conversely, Dini *et al*. [41] showed the use of photofunctionalization with UV light on Ti surfaces stored in contact with ambient air. Their results of wettability characterization results corroborate the present results, where hydrophilicity has been gradually weakening over time when UV light is used [41].

Our *in vitro* results showed similarities in relation to the significantly better osteoblast adhesion and viability on the more hydrophilic anodized surface, resulting from greater cell spread and adhesion on the surface, generating greater contact between cell nanostructures and biomaterial along with intercellular interaction [39,40,42]. After a short duration of contact between the osteoblasts and titanium, microscopic images demonstrate intercellular interaction via filopodia [43]. In our study, after 10 days, we showed that the development of filopodia on a greater scale only on the anodized surface immersed in DI water, suggesting

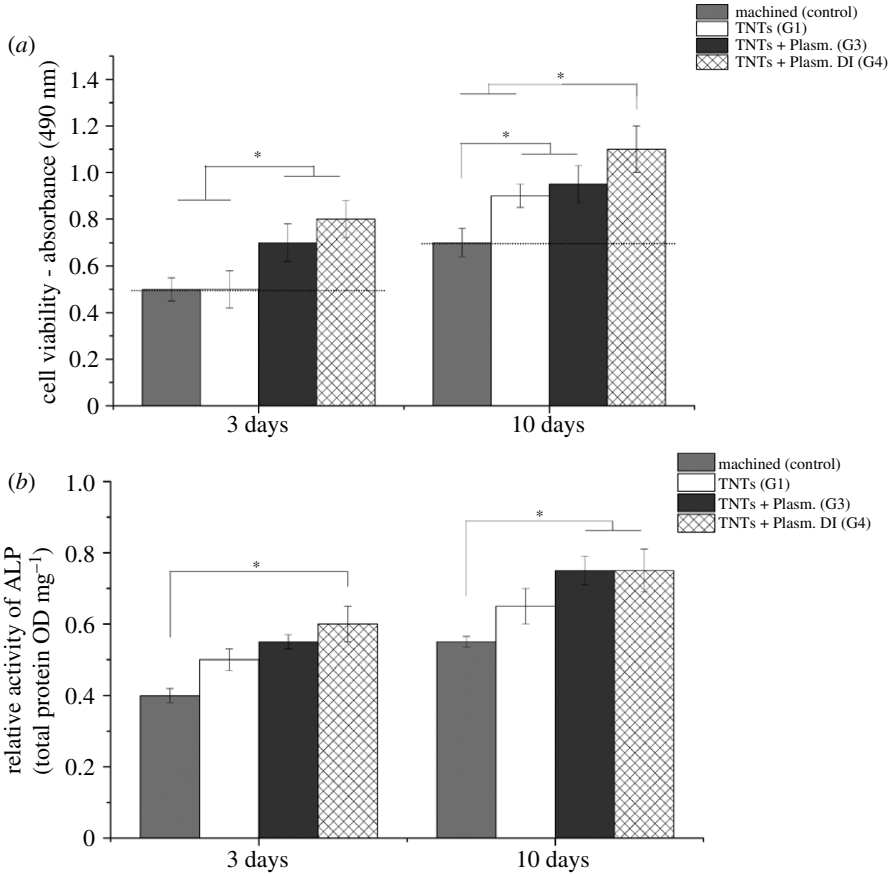

Figure 6. Statistical significance between groups from cell viability (*a*) and alkaline phosphatase (*b*), after 3 and 10 days. *($p < 0.05$) represents significance compared to the indicated groups.

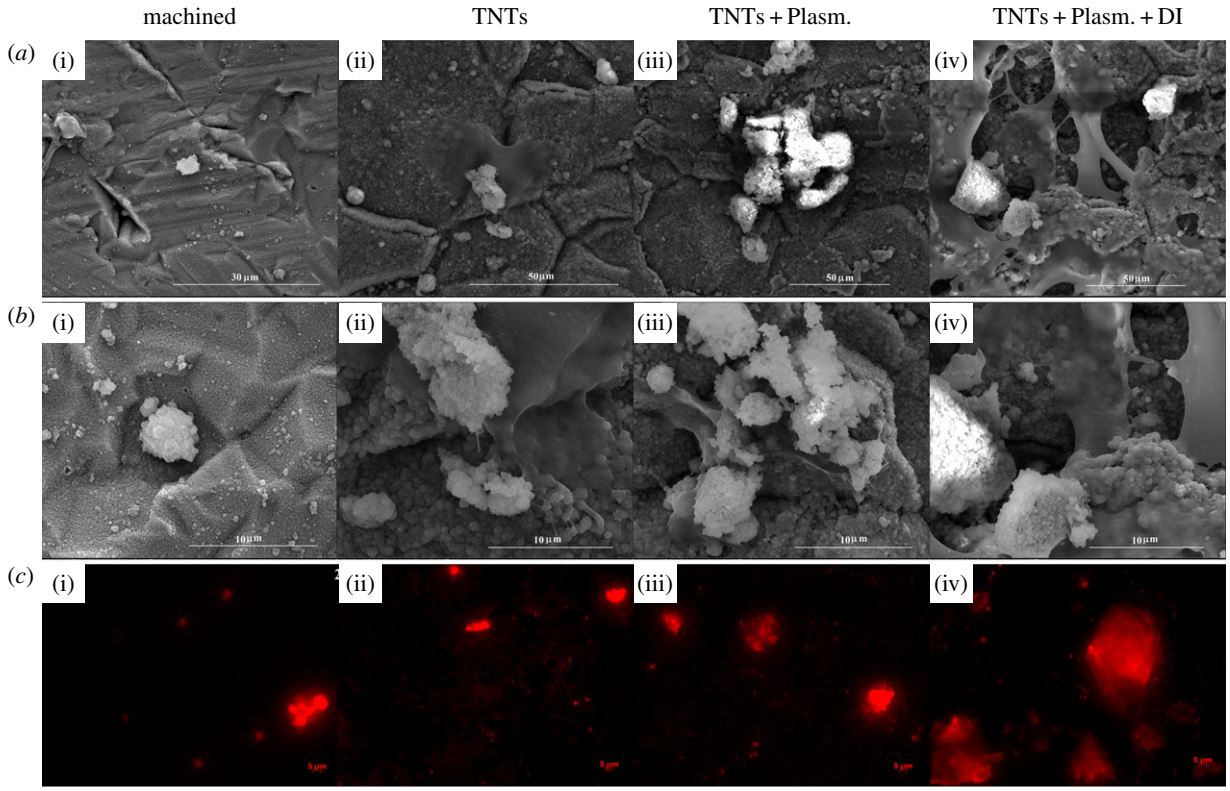

Figure 7. Cell adhesion and bone formation on low—30/50 µm scale bar (*a*) and high—10 µm scale bar (*b*) magnifications. SEM images (*a* and *b*) and confocal microscopy images—5 µm scale bar (*c*).

that maintenance of hydrophilicity is an important factor in cell adhesion.

Another important beneficial characteristic of anodization reported in the literature is related to the possibility of developing a nanoporous surface topography [7,44–47], as can be seen in our study. Surfaces with this superficial design have shown excellent osteogenic responses [7,44], fibroblast alignment/orientation [45] and antibacterial responses [44,46].

The physical structure of the surface also demonstrated better mechanical performance due to the more robust formatting of the TiO_2 nanotubes [47]. In addition, a surface composed of nanotubes with high hydrophilicity allows the incorporation of drugs or nanoparticles that can critically potentiate cell behaviour as reported by several studies [8,48,49]. However, the aim of this study was to verify only the wettability properties without the possible interference of molecules or drugs with different hydrophilic or hydrophobic properties [48,50] that could alter the results.

The limitations of the present study are that it does not allow extrapolations to clinical applications, as it is necessary to perform quantitative adhesion analysis, genetic expression and *in vivo* tests in future studies. Nevertheless, based on studies of high-hydrophilicity implants [51,52], the use of the present methodology to alter the crystalline phase of the surface of titanium implants, comprising an Ar/O_2 plasma treatment of anodized titanium, which is then stored in DI water, suggests a significant improvement in bone cell behaviour, justifying its potential application in biomedical implants.

5. Conclusion

A reactive plasma system was developed and employed to improve surface properties. Therefore, the combination of the anodizing process followed by reactive plasma promotes a surface with nanomorphology, hydrophilicity, roughness alterations and apparent anatase crystallinity. The reactive plasma methodology changes the crystalline phase of the amorphous Ti surface to anatase in a short time with no alterations in surface nanomorphology. Finally, the constant hydrophilicity is only acquired with partial ageing inhibition through immersion in a liquid solution. Together, these characteristics promote better cell morphology, superior viability and significantly higher ALP activity, encouraging this surface treatment for applications in biomedical implants with rapid osseointegration.

Ethics. The present study was approved by the Ethics Committee for Animal Research of the Pontifical Catholic University of Rio Grande do Sul (protocol no. 7467) following all regulations for animal use (Brazilian Regulation no. 11.794, October 2008) according to Ethical Principles in Animal Experimental Research.

Data accessibility. All supporting data, materials, and methodologies are included in this manuscript; moreover, any additional questions can be reported to the corresponding author.

Authors' contributions. M.F.K. was involved in conceptualization, creation, data curation, formal analysis, investigation, methodology, validation, visualization, writing, editing and review; A.L.M.V. was involved in the investigation, methodology, validation, writing and review; P.S. was involved in the investigation, methodology and writing; E.R.T. was involved in methodology and supervision; R.H. was involved in formal analysis, investigation, methodology, supervision, validation, writing and review.

Competing interests. We declare we have no competing interests

Funding. This research did not receive any specific grant from funding agencies in the public, commercial or not-for-profit sectors. This study was partially supported by the Brazilian National Council of Research and Development (CNPq)—research grant no. 140903/2016-0.

Acknowledgements. We appreciate the help of IPB—Institute of Biomedical Research—PUCRS in the methodology for the confocal microscopy, technical help in the microscopy laboratory (LABCEEM-PUCRS) and the ion implantation laboratory—UFRGS for the measures in RBS analyses.

References

1. Glauser R, Sennerby L, Meredith N, Rée A, Lundgren A, Gottlow J, Hämmerle CH. 2004 Resonance frequency analysis of implants subjected to immediate or early functional occlusal loading: successful vs. failing implants. *Clin. Oral Implants Res.* **15**, 428–434. (doi:10.1111/j.1600-0501.2004.01036.x)
2. Palmquist A, Omar OM, Esposito M, Lausmaa J, Thomsen P. 2010 Titanium oral implants: surface characteristics, interface biology and clinical outcome. *J. R. Soc. Interf.* **7**(suppl_5), S515–S527. (doi:10.1098/rsif.2010.0118.focus)
3. Prasad S, Ehrensberger M, Gibson MP, Kim H, Monaco Jr EA. 2015 Biomaterial properties of titanium in dentistry. *J. Oral Biosci.* **57**, 192–199. (doi:10.1016/j.job.2015.08.001)
4. Dai X *et al.* 2016 Synergistic effects of elastic modulus and surface topology of Ti-based implants on early osseointegration. *RSC Adv.* **6**, 43 685–43 696. (doi:10.1039/C6RA04772F)
5. Civantos A, Martinez-Campos E, Ramos V, Elvira C, Gallardo A, Abarrategi A. 2017 Titanium coatings and surface modifications: toward clinically useful bioactive implants. *ACS Biomater. Sci. Eng.* **3**, 1245–1261. (doi:10.1021/acsbiomaterials.6b00604)
6. Cunha A, Renz RP, Blando E, de Oliveira RB, Hübler R. 2014 Osseointegration of atmospheric plasma-sprayed titanium implants: influence of the native oxide layer. *J. Biomed. Mater. Res. A* **102**, 30–36. (doi:10.1002/jbm.a.34667)
7. Gulati K, Moon HJ, Li T, Kumar PS, Ivanovski S. 2018 Titania nanopores with dual micro-/nano-topography for selective cellular bioactivity. *Mater. Sci. Eng. C* **91**, 624–630. (doi:10.1016/j.msec.2018.05.075)
8. Kunrath MF, Hübler R, Shinkai RS, Teixeira ER. 2018 Application of TiO_2 nanotubes as a drug delivery system for biomedical implants: a critical overview. *ChemistrySelect* **3**, 11 180–11 189. (doi:10.1002/slct.201801459)
9. Souza JCM, Sordi MB, Kanazawa M, Ravindran S, Henriques B, Silva FS, Aparicio C, Cooper LF. 2019 Nano-scale modification of titanium implant surfaces to enhance osseointegration. *Acta Biomater.* **94**, 112–131. (doi:10.1016/j.actbio.2019.05.045)
10. Choi SH, Jeong WS, Cha JY, Lee JH, Yu HS, Choi EH, Kim KM, Hwang CJ. 2016 Time-dependent effects of ultraviolet and nonthermal atmospheric pressure plasma on the biological activity of titanium. *Sci. Rep.* **6**, 33421. (doi:10.1038/srep33421)
11. Scharnweber D, Schlottig F, Oswald S, Becker K, Worch H. 2010 How is wettability of titanium surfaces influenced by their preparation and storage conditions? *J. Mater. Sci: Mater. in Medicine* **21**, 525–532. (doi:10.1007/s10856-009-3908-9)
12. Lai Y, Huang J, Cui Z, Ge M, Zhang KQ, Chen Z, Chi L. 2016 Recent advances in TiO_2-based nanostructured surfaces with controllable wettability and adhesion. *Small* **12**, 2203–2224. (doi:10.1002/smll.201501837)
13. Sun Y, Sun S, Liao X, Wen J, Yin G, Pu X, Yao Y, Huang Z. 2018 Effect of heat treatment on surface hydrophilicity-retaining ability of titanium dioxide nanotubes. *Appl. Surf. Sci.* **440**, 440–447. (doi:10.1016/j.apsusc.2018.01.136)
14. Choi SH *et al.* 2019 Effect of wet storage on the bioactivity of ultraviolet light- and non-thermal atmospheric pressure plasma-treated titanium and zirconia implant surfaces. *Mater. Sci. Eng. C* **105**, 110049. (doi:10.1016/j.msec.2019.110049)
15. Hirakawa Y, Jimbo R, Shibata Y, Watanabe I, Wennerberg A, Sawase T. 2013 Accelerated bone formation on photo-induced hydrophilic titanium implants: an experimental study in the dog mandible. *Clin. Oral Implants Res.* **24**, 139–144. (doi:10.1111/j.1600-0501.2011.02401.x)
16. Han Y, Chen D, Sun J, Zhang Y, Xu K. 2008 UV-enhanced bioactivity and cell response of micro-arc

oxidized titania coatings. *Acta Biomater.* **4**, 1518–1529. (doi:10.1016/j.actbio.2008.03.005)

17. Park KH, Koak JY, Kim SK, Heo SJ. 2011 Wettability and cellular response of UV light irradiated anodized titanium surface. *J. Adv. prosthodontics* **3**, 63–68. (doi:10.4047/jap.2011.3.2.63)
18. Liu K, Cao M, Fujishima A, Jiang L. 2014 Bio-inspired titanium dioxide materials with special wettability and their applications. *Chem. Rev.* **114**, 10 044–10 094. (doi:10.1021/cr4006796)
19. Wang N, Li H, Lü W, Li J, Wang J, Zhang Z, Liu Y. 2011 Effects of TiO_2 nanotubes with different diameters on gene expression and osseointegration of implants in minipigs. *Biomaterials* **32**, 6900–6911. (doi:10.1016/j.biomaterials.2011.06.023)
20. Li J, Zhao Y. 2012 Biocompatibility and antibacterial performance of titanium by surface treatment. *J. Coatings Technol. Res.* **9**, 223–228. (doi:10.1007/s11998-009-9221-1)
21. Zhang L, Liao X, Fok A, Ning C, Ng P, Wang Y. 2018 Effect of crystalline phase changes in titania (TiO_2) nanotube coatings on platelet adhesion and activation. *Mater. Sci. Eng. C* **82**, 91–101. (doi:10.1016/j.msec.2017.08.024)
22. Gui N, Xu W, Myers DE, Shukla R, Tang HP, Qian M. 2018 The effect of ordered and partially ordered surface topography on bone cell responses: a review. *Biomater. Sci.* **6**, 250–264. (doi:10.1039/c7bm01016h)
23. Priolo F, Rimini E. 1990 Ion-beam-induced epitaxial crystallization and amorphization in silicon. *Mater. Sci. Rep.* **5**, 321–379. (doi:10.1016/0920-2307(90)90003-L)
24. Kitajima H, Ogawa T. 2016 The use of photofunctionalized implants for low or extremely low primary stability cases. *Int. J. Oral Maxillof. Implants* **31**, 439–447. (doi:10.11607/jomi.4054)
25. Soltanzadeh P, Ghassemi A, Ishijima M, Tanaka M, Park W, Iwasaki C, Hirota M, Ogawa T. 2017 Success rate and strength of osseointegration of immediately loaded UV-photofunctionalized implants in a rat model. *J. Prosthetic Dentistry* **118**, 357–362. (doi:10.1016/j.prosdent.2016.11.008)
26. Kunrath MF, dos Santos RP, de Oliveira SD, Hubler R, Sesterheim P, Teixeira ER. 2020 Osteoblastic cell behavior and early bacterial adhesion on macro-, micro-, and nanostructured titanium surfaces for biomedical implant applications. *Int. J. Oral Maxillof. Implants* **35**, 773–781. (doi:10.11607/jomi.8069)
27. da Silva Meirelles L, Chagas telles PC, Nardi NB. 2006 Mesenchymal stem cells reside in virtually all post-natal organs and tissues. *J. cell sci.* **119**, 2204–2213. (doi: 10.1242/jcs.02932)
28. Yu Y *et al.* 2018 Osteogenesis potential of different titania nanotubes in oxidative stress microenvironment. *Biomaterials.* **167**, 44–57. (doi:10.1016/j.biomaterials.2018.03.024)
29. Hardcastle FD. 2011 Raman spectroscopy of titania (TiO_2) nanotubular water-splitting catalysts. *J. Arkansas academy sci.* **65**, 43–48.
30. Taziwa R, Meyer E, Takata N. 2017 Structural and Raman spectroscopic characterization of C-TiO_2 nanotubes synthesized by a template-assisted sol-gel technique. *J. Nanosci. Nanotechnol. Res.* **1**, 1–11.
31. Zhang WF, He YL, Zhang MS, Yin Z, Chen Q. 2000 Raman scattering study on anatase TiO_2 nanocrystals. *J. Physics D: Appl. Physics* **33**, 912. (doi:10.1088/0022-3727/33/8/305)
32. Renz RP, Vargas ALM, Hübler R. 2015 Use of ion-assisted techniques for determining the structure of TiO_2 nanotubes. *Nucl. Instrum. Methods Phys. Res. B* **365**, 3–7. (doi:10.1016/j.nimb.2015.07.083)
33. Sollazzo V *et al.* 2008 Genetic effect of anatase on osteoblast-like cells. *J. Biomed. Mater. Res. Part B* **85**, 29–36. (doi:10.1002/jbm.b.30912)
34. Duske K, Koban I, Kindel E, Schröder K, Nebe B, Holtfreter B, Jablonowski L, Weltmann KD, Kocher T. 2012 Atmospheric plasma enhances wettability and cell spreading on dental implant metals. *J. Clin. Periodontal.* **39**, 400–407. (doi:10.1111/j.1600-051X.2012.01853.x)
35. Fontes ACA, Sopchenski L, Laurindo CA, Torres RD, Popat KC, Soares P. 2020 Annealing temperature effect on tribocorrosion and biocompatibility properties of TiO_2 nanotubes. *J. Bio-and Tribo-Corrosion* **6**, 1–12. (doi:10.1007/s40735-020-00363-w)
36. Ocampo RA, Echeverry-Rendón M, DeAlba-Montero I, Robledo S, Ruiz F, Echeverría Echeverría F. 2020 Effect of surface characteristics on the antibacterial properties of titanium dioxide nanotubes produced in aqueous electrolytes with carboxymethyl cellulose. *J. Biomed. Mater. Res. Part A* 1–18. (doi:10.1002/jbm.a.37010)
37. Roach MD, Williamson RS, Blakely IP, Didier LM. 2016 Tuning anatase and rutile phase ratios and nanoscale surface features by anodization processing onto titanium substrate surfaces. *Mater. Sci. Eng. C* **58**, 213–223. (doi:10.1016/j.msec.2015.08.028)
38. Gittens RA, Scheideler L, Rupp F, Hyzy SL, Geis-Gerstorfer J, Schwartz Z, Boyan BD. 2014 A review on the wettability of dental implant surfaces II: biological and clinical aspects. *Acta Biomater.* **10**, 2907–2918. (doi:10.1016/j.actbio.2014.03.032)
39. Yamamura K, Miura T, Kou I, Muramatsu T, Furusawa M, Yoshinari M. 2015 Influence of various superhydrophilic treatments of titanium on the initial attachment, proliferation, and differentiation of osteoblast-like cells. *Dental Mater. J.* **34**, 120–127. (doi:10.4012/dmj.2014-076)
40. Toita R, Tsuru K, Ishikawa K. 2016 A superhydrophilic titanium implant functionalized by ozone gas modulates bone marrow cell and macrophage responses. *J. Mater. Sci: Mater. in Medicine* **27**, 127. (doi:10.1007/s10856-016-5741-2)
41. Dini C, Nagay BE, Cordeiro JM, da Cruz NC, Rangel EC, Ricomini-Filho AP, de Avila ED, Barão VAR. 2020 UV-photofunctionalization of a biomimetic coating for dental implants application. *Mater. Sci. Eng. C* **110**, 110657. (doi:10.1016/j.msec.2020.110657)
42. Kopf BS, Ruch S, Berner S, Spencer ND, Maniura-Weber K. 2015 The role of nanostructures and hydrophilicity in osseointegration: in-vitro protein-adsorption and blood-interaction studies. *J. biomed. Mater. Res. Part A* **103**, 2661–2672. (doi:10.1002/jbm.a.35401)
43. Lee JW, Lee KB, Jeon HS, Park HK. 2011 Effects of surface nano-topography on human osteoblast filopodia. *Analytical Sci.* **27**, 369. (doi:10.2116/analsci.27.369)
44. Rodriguez-Contreras A, Bello DG, Nanci A. 2018 Surface nanoporosity has a greater influence on osteogenic and bacterial cell adhesion than crystallinity and wettability. *Appl. Surf. Sci.* **445**, 255–261. (doi:10.1016/j.apsusc.2018.03.150)
45. Gulati K, Moon HJ, Kumar PS, Han P, Ivanovski S. 2020 Anodized anisotropic titanium surfaces for enhanced guidance of gingival fibroblasts. *Mater. Sci. Eng. C* **112**, 110860. (doi:10.1016/j.msec.2020.110860)
46. Kunrath MF, Monteiro MS, Gupta S, Hubler R, de Oliveira SD. 2020 Influence of titanium and zirconia modified surfaces for rapid healing on adhesion and biofilm formation of *Staphylococcus epidermidis*. *Archives Oral Biol.* **117**, 104824. (doi:10.1016/j.archoralbio.2020.104824)
47. Li T, Gulati K, Wang N, Zhang Z, Ivanovski S. 2018 Bridging the gap: optimized fabrication of robust titania nanostructures on complex implant geometries towards clinical translation. *J. Colloid Interface Sci.* **529**, 452–463. (doi:10.1016/j.jcis.2018.06.004)
48. Hu Y, Cai K, Luo Z, Xu D, Xie D, Huang Y, Yang W, Liu P. 2012 TiO_2 nanotubes as drug nanoreservoirs for the regulation of mobility and differentiation of mesenchymal stem cells. *Acta Biomater.* **8**, 439–448. (doi:10.1016/j.actbio.2011.10.021)
49. Kunrath MF, Leal BF, Hübler R, de Oliveira SD, Teixeira ER. 2019 Antibacterial potential associated with drug-delivery built TiO_2 nanotubes in biomedical implants. *AMB Express* **9**, 51. (doi:10.1186/s13568-019-0777-6)
50. Lai M, Jin Z, Yang X, Wang H, Xu K. 2017 The controlled release of simvastatin from TiO_2 nanotubes to promote osteoblast differentiation and inhibit osteoclast resorption. *Appl. Surf. Sci.* **396**, 1741–1751. (doi:10.1016/j.apsusc.2016.11.228)
51. Lang NP, Salvi GE, Huynh-Ba G, Ivanovski S, Donos N, Bosshardt DD. 2011 Early osseointegration to hydrophilic and hydrophobic implant surfaces in humans. *Clin. Oral Implants Res.* **22**, 349–356. (doi:10.1111/j.1600-0501.2011.02172.x)
52. Hicklin SP, Schneebeli E, Chappuis V, Janner SFM, Buser D, Brägger U. 2016 Early loading of titanium dental implants with an intra-operatively conditioned hydrophilic implant surface after 21 days of healing. *Clin. Oral Implants Res.* **27**, 875–883. (doi:10.1111/clr.12706)